

# **ELECTROWEAK PHYSICS RESULTS FROM THE SLD**

Frank E. Taylor\*

Laboratory for Nuclear Science  
Massachusetts Institute of Technology  
Cambridge, MA 02139

Representing the SLD Collaboration

## **ABSTRACT**

Data taken by the SLD Collaboration at the Stanford Linear Collider on  $e^+e^- \rightarrow Z^0$  obtained with a polarized electron beam have enabled many incisive tests of the electroweak sector of the standard model to be performed. We discuss our recent determinations of  $\sin^2\theta_w$ , derived from the total cross section asymmetry, and the quark final state asymmetries,  $A_s$ ,  $A_c$ ,  $A_b$  and branching ratios,  $R_c$  and  $R_b$ . Aspects of the precision tests of the standard electroweak theory, involving radiative corrections, are described. Limits on the Higgs particle are given.

---

\* Work supported in part by the Department of Energy.

# 1 INTRODUCTION

The theoretical description of electron-positron annihilation into the  $Z^0$  vector boson is rich with experimentally testable predictions. Since the first data taken at LEP and SLC in 1990, experimental tests have been made of the standard model (SM) with ever increasing statistical and systematic precision. The data have been for some time of sufficient quality to probe the radiative corrections related to the top quark and Higgs particle. To date, no experimental test of the standard model has shown a persistent and confirmed deviation from theory. Rather than spectacular anomalies discovered, the experimental program at LEP-I and SLC is characterized as one of ever increasing refinement and verification of theory. At this time, the  $Z^0$ -pole data in conjunction with measurements at the FNAL collider of the  $W^\pm$  boson and top quark masses, are beginning to approach the untested Higgs sector of the theory.

The SLD-SLC facility<sup>1</sup> brings a number of unique features to the exploration of the Standard Model (SM) at the  $Z^0$  - pole. The SLC produces  $Z^0$ s with polarized electrons colliding with unpolarized positrons in an exquisitely small intersection region that is roughly  $1.6 \mu\text{m}^2$  ( $700 \mu\text{m}$ ) transverse (longitudinal) to the beam. The electron polarization provided by the SLC allows a quite precise measurement of  $\sin^2\theta_w$  to be made with a statistical 'boost' proportional to  $1/|P_e|^2$ , where  $P_e$  is the electron polarization using the total cross section left-right asymmetry,  $A_{LR}$ . Tests of the SM can be performed on measurements of the properties of the final state, such as a study of the forward-backward left-right cross section asymmetry for b-quark final states. The SLD is equipped with a pixel vertex detector, based on the CCD technology, which is used to identify b- and c-quark final states and a Cherenkov ring imaging detector (CRID) for particle ID. The vertex detector has been recently upgraded, permitting better vertex resolution and coverage<sup>2</sup>.

Table 1: History of SLD data taking.

Year	Purpose	Events	e <sup>-</sup> Polarization
1992	physics	10k	22 %
1993	physics	50k	63 %
1994-5	physics	100k	77 %
1996	physics & VXD3 commissioning	50k	77 %
1997-8	physics	350k	73 %

Table 1 is a summary of the data taken at the SLD. Noteworthy is the outstanding accelerator operation during 1997-8, when the SLC delivered up to 20k polarized  $Z^0$  events in a week. The total number of polarized  $Z^0$  events is 560k with an 'event-weighted' polarization of  $\sim 72\%$ .

## 2 Basics of The Standard Model

For leptons at lowest order, the  $SU(2)_L \times U(1)$  standard model of Glashow-Weinberg-Salam<sup>3</sup> has the following Feynman rules for the neutral current (NC) and charged current (CC) fermion-gauge boson interactions, written in terms of the members of the first generation:

(a)  $\gamma$  -  $e^+e^-$  interactions ( $NC_\gamma$ ):

$$-iQ_e \bar{e} \gamma_\lambda e, \quad (1a)$$

(b)  $Z^0$  -  $f\bar{f}$  ( $f = e, \nu$ ) interactions ( $NC_Z$ ):

$$\frac{-i}{\sqrt{2}} \left( \frac{G_F M_Z^2}{\sqrt{2}} \right)^{1/2} \bar{f} \gamma_\lambda (g_V^f - g_A^f \gamma_5) f, \quad (1b)$$

(c)  $W^\pm$  -  $e\nu$  interactions (CC):

$$-i \left( \frac{G_F M_W^2}{\sqrt{2}} \right)^{1/2} \nu \gamma_\lambda (1 - \gamma_5) e, \quad (1c)$$

where  $G_F$  is the fermi coupling constant,  $M_Z$  the Z-boson mass and  $g_V$ ,  $g_A$  are NC vector and axial vector coupling constants, respectively. The two NC interactions, involving the exchange of  $\gamma$  or  $Z$ , are characterized by coupling strengths  $e$  and  $g'$ , respectively, whereas the charged current (exchange of  $W^\pm$ ) has a coupling strength  $g \sim \sqrt{G_F} M_W$ . The coupling constants involving the exchange of massive vector bosons ( $W^\pm$  and  $Z^0$ ) are related by the Weinberg mixing angle,  $\theta_w$ , with  $\tan\theta_w = g'/g$  and the electromagnetic neutral current is 'unified' with the  $W^\pm$  and  $Z$  interactions by  $e = g'g/\sqrt{g'^2+g^2}$ . The NC interaction for a massive fermion pair coupled to the  $Z^0$  has generally unequal right and left terms couplings  $g_{Re}$  and  $g_{Le}$ , respectively. The CC interaction is pure 'V-A'.

By the Higgs mechanism the vector boson masses,  $M_w$  and  $M_Z$ , acquire mass of magnitude determined by the vacuum expectation value of the Higgs field, given by  $\langle v \rangle = (\sqrt{2} G_F)^{-1/2} = 246$  GeV, and the coupling constants  $g$  and  $g'$ . The fermi coupling constant,  $G_F$ , is the only 'dimensioned number' in the theory. It is conventional to express the boson masses in terms of the experimentally determined constants  $\alpha_{em}$ ,  $\sin^2\theta_w$  and  $G_\mu$ , where  $\alpha_{em}$  is the fine structure constant and is determined by the quantum hall effect and Thomson scattering at low energies,  $\sin^2\theta_w$  is measured by a number of experiments and  $G_\mu = G_F$  by precision muon decay data. In this convention we have:

$$M_Z^2 = \frac{\pi \alpha_{em}}{\sqrt{2} G_\mu \sin^2\theta_w \cos^2\theta_w \zeta_Z} \quad (2a)$$

$$M_W^2 = \frac{M_Z^2}{2} \left( 1 + \sqrt{1 - \frac{4\pi \alpha_{em}}{\sqrt{2} G_F \zeta_w M_Z^2}} \right), \quad (2b)$$

where  $\zeta_Z$  and  $\zeta_w$  are radiative correction terms, of order 1, to be described later. The NC vector and axial vector couplings (or right and left-handed couplings) for fermion,  $f$ , are given by:

$$g_{Vf} = (g_{Lf} + g_{Rf}) = I_{Lf}^3 - 2Q_f \sin^2\theta_w \quad (3a)$$

$$g_{Af} = (g_{Lf} - g_{Rf}) = I_{Lf}^3, \quad (3b)$$

respectively, where  $I_{Lf}^3$  is the third component of fermion,  $f$ , weak isospin and  $Q_f$  is the corresponding electric charge. Since most of the precision electroweak data are at the  $Z$  pole it is conventional to take  $\sin^2\theta_w^{\text{eff}}$  to be the *effective value* at the pole<sup>4</sup>, thereby absorbing the radiation corrections in the gauge boson propagators. As such,

$$\sin^2\theta_w^{\text{effective}} = (1 - g_{Vf}/g_{Af}) / 4|Q_f|, \quad (4)$$

where  $g_{Vf}$  and  $g_{Af}$  are the *effective* vector and axial vector couplings of fermion,  $f$ , at the  $Z^0$  - pole.

Two important measurables at the  $Z^0$  - pole dependent on the coupling of  $Z^0 \rightarrow f \bar{f}$  involve determining the partial decay width given by

$$\Gamma_{ff} = \frac{\sqrt{2} G_m M_Z^3}{12\pi} N_C (g_{Vf}^2 + g_{Af}^2) \zeta_{ff} \quad (5a)$$

where  $N_C$  is the number of color degrees of freedom ( $N_C = 1$  for leptons and 3 for quarks) and  $\zeta_{ff}$  is a radiative correction term, of order 1, and the coupling constant asymmetry, defined as:

$$A_f = \frac{g_{Lf}^2 - g_{Rf}^2}{g_{Lf}^2 + g_{Rf}^2} = \frac{2 g_{Vf} g_{Af}}{g_{Vf}^2 + g_{Af}^2} = \frac{2 g_{Vf} / g_{Af}}{1 + (g_{Vf} / g_{Af})^2}. \quad (5b)$$

The coupling asymmetry for charged leptons is especially sensitive to the effective mixing angle,  $\theta_w^{\text{eff}}$ . Table 1 shows the couplings, asymmetry and sensitivity of the asymmetry to the effective mixing angle for the first generation quarks and leptons.

Table 2: First Generation Coupling constants and sensitivity of  $A_f$  to  $\sin^2\theta_w^{\text{eff}}$  for  $\sin^2\theta_w^{\text{eff}} = 0.23$ .

f	$I_{Lf}^3$	$Q_f$	$g_{Af}$	$g_{Vf}$	$g_{Lf}$	$g_{Rf}$	$A_f$	$\frac{\delta A_f}{\delta \sin^2\theta_w}$
$\nu$	1/2	0	1/2	1/2	1/2	0	1	0
e	-1/2	-1	-1/2	-0.04	-0.27	0.23	0.16	-7.9
u	1/2	2/3	1/2	0.19	0.35	-0.16	0.69	-3.5
d	-1/2	-1/3	-1/2	-0.35	-0.43	0.08	0.94	-0.6

Eqs. 1, 2 and 3, with radiative corrections, form the basis of precision tests of the electroweak sector of the SM and eqs. 4, 5 and Table 1 furnish the tools and predictions of the SM. Note that the charged lepton couplings (e,  $\mu$ ,  $\tau$ ) are dominated by the axial term and have the greatest sensitivity for the determination of  $\sin^2\theta_w$  and that the down quark couplings (d, s, b) are similar, but opposite sign, to the neutrino couplings and have a small sensitivity to  $\sin^2\theta_w$ . As a consequence, the down-like quark couplings lead to their being strongly polarized left-handed in  $Z^0$  decay.

Some of the questions we have addressed to the data are:

- Is the Lorentz structure of the electroweak interaction described correctly by eq. 1 ?
- Are the couplings for all generations and weak isospin states given by the theory isospin assignments and a *universal value* of  $\sin^2\theta_w^{\text{eff}}$  ?
- Are the physical gauge boson masses related by eq. 2 ?
- Do the higher order radiative corrections result in better consistency of the data ?

## 2.1 Measurement of Weak Couplings

One of the fundamental tests of the SM afforded by data at the  $Z^0$  pole is the check of the  $SU(2)_L \times U(1)$  gauge group structure of the theory. It is of interest to see if eqs. 3, 4 and 5 and the weak isospin and charge assignments of Table 1 are operative for all generations with the *same value* of  $\sin^2\theta_w^{\text{eff}}$ . This test is sensitive to putative  $Z^0$ 's, indicating a new gauge group, or, as yet unobserved, new particles which could lead to non-universal radiative corrections for different generations.

In the context of the SM the differential cross section for  $e^+ e^- \rightarrow Z^0 \rightarrow f \bar{f}$ , in the case, for example, of a left-handed electron producing a left-handed fermion in the final state, has the form

$$\sigma(\cos\theta) \sim g_{Le}^2 g_{Lf}^2 (1 + \cos\theta)^2, \quad (8)$$

where  $\theta$  is the angle of the final fermion with respect to the electron beam direction and  $g_{Le}$  and  $g_{Lf}$  are the left-handed electron and final fermion couplings to  $Z^0$ , respectively. Averaging over final fermion helicities for an electron beam with a polarization of  $P_e$ , the differential cross section has the form

$$\frac{d\sigma}{d\cos\theta} \sim (1 - P_e A_e) (1 + \cos\theta)^2 + 2\cos\theta (A_e - P_e) A_f. \quad (9)$$

Here the electron and final fermion coupling asymmetry parameters  $A_e$ ,  $A_f$  are given by eq. 5b.

Fig. 1 shows the differential cross section for the production of  $b \bar{b}$  for three electron beam polarization cases. Note that for left-handed incident electrons the  $b$ -quark tends to go in the forward hemisphere. This large production asymmetry is ex-

exploited by the SLD in b-quark studies in tests of the SM through electroweak coupling asymmetries and b-quark flavor mixing.

The basis of the measured asymmetries at LEP and SLC is given by Eqs. 10. At LEP the forward-backward asymmetry ( $P_e = 0$ ), given by

$$A_{\text{FB}}^f = \frac{\sigma_{\text{F}}^f - \sigma_{\text{B}}^f}{\sigma_{\text{F}}^f + \sigma_{\text{B}}^f} = \frac{3}{4} A_e A_f, \quad (10a)$$

is a measure of the product of coupling asymmetries  $A_e A_f$ . The forward-backward asymmetry is exploited at LEP to obtain lepton and quark couplings.

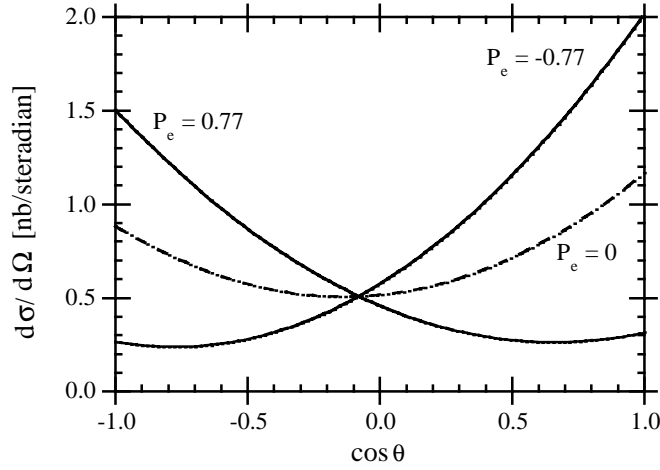


Figure 1: The differential cross section for  $e^+e^- \rightarrow Z^0 \rightarrow b \bar{b}$  is shown for  $P_e = \pm 0.77$ , corresponding to polarized electron beams at SLC and  $P_e = 0$ , the operating condition for LEP.

The left-right total cross section asymmetry, exploited by the SLD Collaboration<sup>5</sup>, is given by

$$A_{\text{LR}} = \frac{\sigma_{\text{L}} - \sigma_{\text{R}}}{\sigma_{\text{L}} + \sigma_{\text{R}}} = |P_e| A_e, \quad (10b)$$

where  $\sigma_{\text{L,R}}$  are the  $e^+ e^- \rightarrow Z^0$  total cross sections for incident L, R electron polarizations and is the *centerpiece* of our precision electroweak tests at the SLC. Knowledge of the electron polarization  $|P_e|$  allows the electron  $Z^0$  coupling

asymmetry,  $A_e$ , to be directly and quite accurately measured. The polarized forward - backward asymmetry, given by

$$A_{\text{FB\_LR}}^f = \frac{(\sigma_{\text{FL}}^f - \sigma_{\text{BL}}^f) - (\sigma_{\text{FR}}^f - \sigma_{\text{BR}}^f)}{\sigma_{\text{FL}}^f + \sigma_{\text{BL}}^f + \sigma_{\text{FR}}^f + \sigma_{\text{BR}}^f} = \frac{3}{4} |P_e| A_f, \quad (10c)$$

allows a *direct determination* of the final state fermion coupling asymmetry parameters,  $A_f$ . This asymmetry is used at the SLC to measure  $A_b$  and  $A_c$ .

The  $\tau$ -lepton polarization is measured both at LEP and SLC, by, for example, the energy distribution of the  $\pi$  in  $\tau^- \rightarrow \pi^- \nu_\tau$  decay. By the SM the  $\tau$ -polarization,  $P_\tau(\cos\theta)$ , is dependent on both  $A_\tau$  and  $A_e$  by

$$P_\tau(z) = - \frac{(1+z^2)(1+A_e P_e) A_\tau + 2(A_e + P_e) z}{(1+z^2)(1+A_e P_e) + 2(A_e + P_e) A_\tau z}, \quad (10d)$$

where  $z = \cos\theta$  and  $\theta$  is the angle between the  $\tau$ -lepton and the electron beam direction and  $P_e$  is the incident electron beam polarization ( $P_e = 0$  at LEP). Both LEP and SLD have determined  $A_e$  and  $A_\tau$  by this method. The SLD collaboration exploits the polarized incident electron beam<sup>6</sup> to measure an asymmetry enhanced by a large factor ( $\sim 3.4$  at large  $|\cos\theta|$ ).

### 3 Lepton Asymmetries

Lepton asymmetries derived from pure leptonic final states  $Z^0 \rightarrow l^+ l^-$  are the easiest to interpret as precision tests of the SM. Nevertheless, the b-quark asymmetry, exploited by the LEP experiments, offers a high statistical precision method within the context of the SM for determining the electron asymmetry,  $A_e$ .

#### 3.1 Pure Lepton Modes

The single most precise determination of the electron asymmetry and thus of  $\sin^2\theta_w^{\text{eff}}$  comes from the measurement at the SLD of the total  $e^+e^-$  cross section asymmetry  $A_{\text{LR}}$ , defined by eq. 10b. The measurement directly determines  $A_e$ , the electron coupling asymmetry, with only small corrections and is only possible with incident polarized beams. Events for the  $A_{\text{LR}}$  analysis are selected to be 'hadronic' and

not a beam background,  $2\gamma$  or Bhabha event. Small experimental corrections of order  $\sim 0.3\%$  are made for backgrounds, experimental asymmetries and direct channel  $\gamma$ -exchange and  $Z^0 \gamma$ -interference. The systematic error of the measurement of  $A_{LR}$  is dominated by the electron beam polarization uncertainty. The electron beam polarization is directly measured by means of a Compton polarimeter<sup>1</sup> throughout data taking, with running averages updated at least as frequently as every hour giving rise to an estimated systematic error presently at the level of  $\Delta P_e/P_e \sim 0.7\%$  for the 94-95 period and  $\sim 1.1\%$  for 97-98 data.

The lepton coupling asymmetry parameters  $A_L$ , for  $L = e, \mu,$  and  $\tau$  have been directly measured<sup>7</sup> using corresponding *lepton final states* by the FB-LR asymmetry of eq. 10c. The resulting cross sections are shown in Fig. 2. Although of limited statistics ( $e, \mu, \tau$ : 9.4k, 7.6k, 7.1k events) this test is a direct measurement of  $A_\mu$  and  $A_\tau$ , a confirmation of  $A_e$  using the electron final state and a probe of lepton universality. A maximum likelihood method is used to determine the coupling asymmetries which takes into account all known cross section terms (10 terms for the  $e^+e^-$  final state), backgrounds and detection efficiencies.

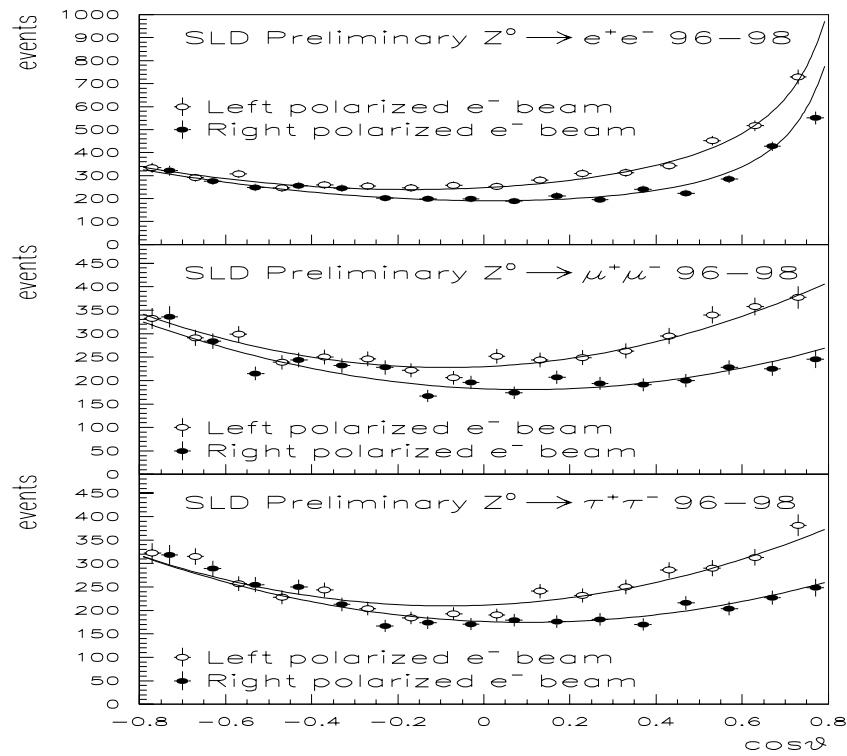


Figure 2: The differential cross section measured at the SLD for  $e^+ e^- \rightarrow Z^0 \rightarrow e^+ e^-$ ,  $\mu^+ \mu^-$  and  $\tau^+ \tau^-$  are shown.

At the end of the 97-98 run several important checks of the SLC parameters were performed which are important to certify the small corrections of  $\gamma$  exchange and  $\gamma$ - $Z^0$  interference and to make certain that the SLC positrons are not polarized. In order to check the energy calibration of the electron and positron spectrometers, which follow the beam interaction point, the  $Z^0$  cross section peak was scanned and matched to the  $Z^0$  mass determined at LEP-I. It was determined that the energy scale is known to about 40 MeV which results in a negligible correction in  $\sin^2 \theta_w^{\text{eff}}$  ( $0.00011 \pm 0.00009$ ). In addition, a putative positron polarization was sought by directly measuring the positron beam polarization by means of a Møller polarimeter located in end station A and found to be consistent with zero ( $P_{e^+} = -0.02 \pm 0.07\%$ ). Finally, the Compton polarimeter, which measures the electron polarization, was questioned but found to be in good agreement with measurements of the energy asymmetry of back-scattered Compton gammas detected by a threshold Cherenkov gas counter and a quartz fiber - tungsten radiator calorimeter.

In Table 3 we summarize the world's data on lepton coupling asymmetries<sup>7,8</sup> (both SLD<sup>7</sup> and LEP<sup>8</sup> data are preliminary).

Table 3: Lepton Coupling Asymmetries.

Quantity	Asymmetry
SLD: $A_{LR}$	$0.1510 \pm 0.0025$
SLD: $A_e$	$0.1504 \pm 0.0072$
SLD: $A_\mu$	$0.120 \pm 0.019$
SLD: $A_\tau$	$0.142 \pm 0.019$
SLD: $\langle A_{e,\mu,\tau} \rangle$	$0.1459 \pm 0.0063$
SLD: $A_{LR}, \langle A_{e,\mu,\tau} \rangle$	$0.1503 \pm 0.0023$
LEP: $AFB(l), A_{e,\mu,\tau}$	$0.1469 \pm 0.0027$
SLD+LEP	$0.1489 \pm 0.0018$

We note that the LEP-I values and those from the SLC-SLD are in good agreement with the resulting value of leptonic asymmetries differing by only  $\sim 1 \sigma$ .

### 3.2 $A_e$ from b-Quark Asymmetry

The experiments at LEP have exploited  $Z^0 \rightarrow b \bar{b}$  data to determine  $A_{\text{FB}}^{0b}$ , the b-quark asymmetry at the pole, and hence  $A_e$  within the context of the SM. [See eq. 10a.] The method rests on the assumption that  $A_b$ , the asymmetry parameter of the b-quark coupling, agrees with the SM prediction since what is actually measured in  $A_{\text{FB}}^{0b}$  is the product of  $A_b A_e$ . Even within the context of the SM, important corrections are needed before an accurate value of  $A_e$  can be extracted from  $A_{\text{FB}}^{0b}$ . The c-quark background can dilute the b-asymmetry since this background enters with a smaller asymmetry and opposite electric charge. The jet charge method is especially sensitive to this correction. QCD effects, which tend to smear the direction of the final state quarks and make the measured asymmetry smaller, and  $B - \bar{B}$  flavor mixing are two other corrections which must be included. The resulting  $A_{\text{FB}}^{0b}$  measurement from LEP is  $0.0991 \pm 0.0021$ . Using the SM model value of  $A_b = 0.935$ , the corresponding value of  $A_e = 0.14145 \pm 0.0030$ , which is  $2.1 \sigma$  different from the pure lepton-based determinations above<sup>7</sup>.

### 4 Determination of $\sin^2 \theta_w^{\text{eff}}$

Through eqs. 3 and 5b the value of  $\sin^2 \theta_w^{\text{eff}}$  can be determined. The results are given in Table 4. The right-most column indicates the  $\chi^2/\text{DoF}$  of the LEP measurements alone and of the LEP and SLC preliminary measurements combined. We take these data to be in generally good agreement, although we note that the pure leptonic - derived values of  $\sin^2 \theta_w^{\text{eff}}$  measured at the SLC and LEP are smaller than value derived from  $A_{\text{FB}}^{0b}$  at LEP.

Table 4: Effective mixing angle at the  $Z^0$ -pole.

Measurement	$\sin^2 \theta_w^{\text{eff}}$	$\chi^2/\text{DoF}$
SLC: $A_{\text{LR}}, \langle A_{e,\mu,\tau} \rangle$	$0.23110 \pm 0.00029$	
LEP: $A_{\text{FB}}^{0l}$	$0.23117 \pm 0.00054$	
LEP: $A_\tau$	$0.23202 \pm 0.00057$	
LEP: $A_e$	$0.23141 \pm 0.00065$	
LEP leptonic	$0.2316 \pm 0.0004$	1.2/2

SLC+LEP leptonic	$0.23127 \pm 0.00023$	
LEP: $A_{FB}^{0b}$	$0.23223 \pm 0.00038$	
LEP: $A_{FB}^{0c}$	$0.2320 \pm 0.0010$	
LEP: $\langle Q_{FB} \rangle$	$0.2321 \pm 0.0010$	
LEP average	$0.23187 \pm 0.00024$	3.2/5
LEP+SLC average	$0.23156 \pm 0.00018$	7.3/6 all

The  $\chi^2/\text{DoF}$  of all data is 7.3/6 ( $\sim 32\%$  CL), whereas for only lepton-based

measurements  $\chi^2/\text{DoF} = 3.7/3$  ( $\sim 35\%$  CL) - both reasonable agreement. Later, we make an observation on the nature of the  $\sin^2\theta_w^{\text{eff}}$  value derived from  $A_{FB}^{0b}$  at LEP and the experimental value of  $A_b$ .

## 5 Standard Model Tests with s, c and b Quarks

It is interesting to see if the coupling constants  $g_V$  and  $g_A$  for the s-, c- and b-quarks follow the predictions of the SM. Two variables are accessible for this test of the SM: the coupling constant asymmetry and the branching ratio. The coupling constant asymmetry measures the combination  $A_f = 2g_{Vf}/g_{Af}/(1 + (g_{Vf}/g_{Af})^2)$  and the branching ratio for  $Z^0$  to decay into a quark favor, f, determines the combination  $R_f = \Gamma_f/\Gamma_{\text{had}} \sim (g_{Vf}^2 + g_{Af}^2)$ . To check theory, the vector and axial vector couplings are taken from either the average value of  $\sin^2\theta_w^{\text{eff}}$  derived from global fits, where the overall consistency of the data is checked. Or more strictly, the value of  $\sin^2\theta_w^{\text{eff}}$  is taken from purely lepton measurements, thereby probing the universality of  $\sin^2\theta_w^{\text{eff}}$  across lepton-quark families. In the case of the  $Z^0 \rightarrow b \bar{b}$  vertex (also  $Z^0 \rightarrow s \bar{s}$ ), since  $g_L^2 \sim 30 g_R^2$ ,  $R_b$  has a large sensitivity to the *left-handed* coupling, such as vertex corrections involving  $W^\pm$ ,  $t^\pm$  exchange, whereas  $A_b$  has a greater sensitivity to the *right-handed* components. We find the following sensitivities for  $\sin^2\theta_w^{\text{eff}} \cdot 0.23$

$$\frac{\delta R_b}{R_b} \sim -3.6 \delta g_{Lb} + 0.7 \delta g_{Rb} \quad (11a)$$

$$\frac{\delta A_b}{A_b} \sim -0.3 \delta g_{Lb} + 1.7 \delta g_{Rb} \quad (11b)$$

Thus,  $R_b$  and  $A_b$  are complementary measurements and probe different sectors of theory.

The SLD brings a number of experimental tools to the study of the electroweak couplings of s, c and b-quarks. The pixel vertex detector and identify displaced vertices from the IP as a signature for b and c quark final states and the Cherenkov Ring Imaging Detector (CRID) can identify  $\pi^\pm$ ,  $K^\pm$ ,  $p^\pm$  particles in the final state. Various discriminates are used to isolate s-, c-, b-quark events which result for example in a hemisphere b-tag efficiency and purity in the range of 45% and 99%, respectively.

The most powerful test of the SM for quark final states of come from a study of the b-system. Several factors conspire to allow this.

- (1) The asymmetry parameter  $A_b$  is expected to be only weakly dependent on  $\sin^2\theta_w^{\text{eff}}$  (see the entry for d-quarks in Table 1), thus the measurement of  $A_{\text{FB}}^b$ , given by eq.10a, is mostly a determination of  $A_e$ .
- (2) The b-quark has a large branching ratio (~22%) and thus has a small statistical error for reasonable detection efficiency.
- (3) b-quark events can be separated from other hadronic events by detection of displaced secondary vertices and various event attributes, such as high transverse mass.
- (4) The b-quark charge can be determined by a variety of experimental signatures, such as high  $P_t$  charged lepton, jet charge, kaon charge and, in the SLD, initial state tagging through the incident electron beam polarization.
- (5)  $A_{\text{FB}}$  varies with center-of-mass energy and when measured below and above the  $Z^0$  peak at LEP has a larger asymmetry, thereby adding information to the small asymmetry at the pole.

Similar arguments hold for s-quark and c-quark final states (no flavor mixing), although the c-quark final state is more sensitive to  $\sin^2\theta_w$ , thereby making the test of the SM more involved. Further, c-quarks are more difficult to separate from background and their detection frequently exploits 'charm counting' where all charm hadrons which eventually decay via  $D^0$ ,  $D^+$ ,  $D_s$ ,  $\Lambda_c$  are summed, or by the

reconstruction of  $D^*$ s, yielding a clean sample of events. A lepton fit is also used to separate  $c$  (and  $b$ ) events from background.

The coupling constant asymmetry measurements are not sensitive to the detection efficiency, although the background dilution in the asymmetry is. For the branching ratio analysis the detection efficiency critically enters and it is highly beneficial to achieve high detection efficiency since, for example,  $\delta R_b \sim 1/\epsilon_b$ .

## 5.1 Measurements of $A_s$ , $A_c$ and $A_b$

The SLD has measured  $A_s$ ,  $A_c$  and  $A_b$  directly through eq. 10c, which depends critically on a precise knowledge of the electron beam polarization,  $P_e$ , but is a direct and powerful method largely independent of the  $Z^0$ -leptonic coupling physics<sup>9, 10, 11</sup>. Fig. 3 shows the left and right asymmetries as determined by jet-charge for  $b$ -quarks as observed by the SLD<sup>11</sup>. (See Fig. 1 for the relevant physics at the tree-level.) LEP derives the asymmetry parameters by the forward-backward composite asymmetry,  $A_{FB}$ , given by eq. 10a. For the extraction of  $A_b$  and  $A_c$  using  $A_{FB}$ , a value of  $A_e$  derived from other measurements must be used.

The resulting asymmetries determined at LEP and SLC are given in Tables 5, 6 and 7 for  $A_s$ ,  $A_c$  and  $A_b$ , respectively. The LEP  $A_{FB}$  asymmetries have been corrected by the factor  $4 / (3 A_e)$  with  $A_e = 0.1491 \pm 0.0018$  (average of  $A_{LR}$  and LEP leptonic). In the tables the combined averages have taken into account correlations between measurements.

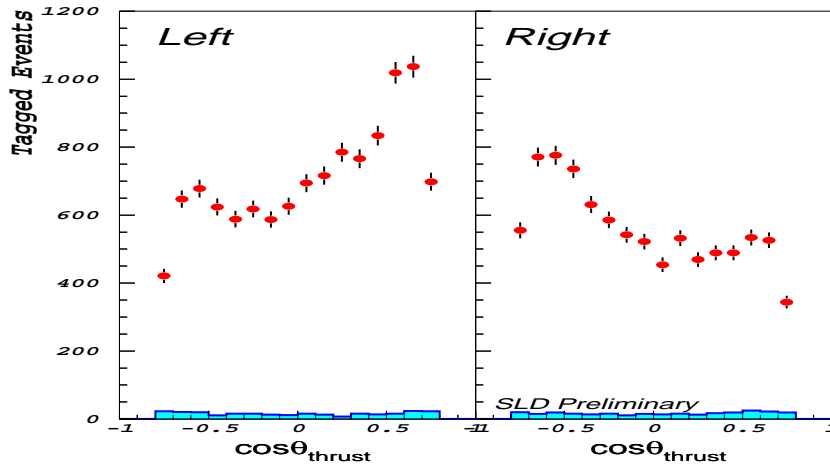


Figure 3: The  $\theta$ -angle distribution for b-quarks produced from left and right electron beam polarizations at the SLD indicating the forward-backward left-right asymmetry in b-quark production as measured by the jet-charge asymmetry.

The SLD determination of  $A_s$  is derived from a sample of approximately 300 k hadronic decays of  $Z^0$  bosons produced with a polarized electron beam. The  $s\bar{s}$  sample was selected by suppressing heavy quark decays (c and b) by requiring well-reconstructed tracks to have a transverse impact parameter with the IP to be less than the 3 times the estimated resolution. The impact parameter resolution obtained from our upgraded CCD vertex detector, VXD3, is given by  $\sigma_d = 9 \oplus 29(p_{\perp} \sin^{3/2} \theta) \mu\text{m}$ , where  $\theta$  is the polar angle of the track with respect to the beam. Further refinements of the  $s\bar{s}$  sample were obtained by using the Cherenkov Ring Imaging Detector (CRID) to identify  $K^{\pm}$ . In addition,  $K_s^0$  and  $\Lambda^0/\bar{\Lambda}^0$  were reconstructed and employed as tags of  $s\bar{s}$  final state.

Table 5:  $A_{d,s}$  measurements from LEP and SLC (Summer-1998).

Experiment	Method	Asymmetry
SLD	$A_s$	$0.82 \pm 0.10 \pm 0.07$
DELPHI: (1995)	$A_s$	$1.165 \pm 0.311 \pm 0.116$
DELPHI: (1995)	$A_{d,s}$	$0.996 \pm 0.276 \pm 0.480$
OPAL: (1997)	$A_{d,s}$	$0.605 \pm 0.311 \pm 0.098$
LEP average		$0.91 \pm 0.21$
LEP+SLD average		$0.84 \pm 0.10$

Each of two hemispheres, defined by the perpendicular plane bisecting the thrust axis, was required to have at least one identified strange particle. Overall, the purity of the  $s\bar{s}$  final state was estimated to be 69% with 10%  $u\bar{u}$ , 9%  $d\bar{d}$ , 11%  $c\bar{c}$  and 1%  $b\bar{b}$  contamination. A binned maximum likelihood fit was performed to determine  $A_s$ . The procedure included particle detection efficiencies and acceptances.

Taking  $\sin^2\theta_w^{eff} = 0.23155$ , the SM predicts  $A_s = 0.935$ , a value which is slowly varying with  $\sin^2\theta_w^{eff}$ . The table indicates that the preliminary SLC value of  $A_s$  is 1.0

$\sigma$  low with respect to the SM and the LEP value is 0.1  $\sigma$  low (with  $A_e$  correction made). The SLD+LEP average is dominated by the SLC value and is 1.0  $\sigma$  low.

The SLD brings an excellent vertex detector and particle identification to the isolation of  $c\bar{c}$  events. From the ensemble of hadronic events secondary vertices possibly signifying  $c\bar{c}$  events are identified by means of a topological algorithm<sup>12</sup> which searches for space points in 3 dimensions where the reconstructed tracks overlap. Tracks, in this algorithm, are considered probability 'tubes'. The method finds secondary vertices in 84% of b, 38% of c and 2% of light quark events under the requirement that the secondary vertex be displaced from the IP by at least 1 mm. Further refinement of the charm sample is obtained by reconstructing the mass of the tracks associated with the secondary vertex - a calculation aided by the well-defined IP of the SLC and our high resolution pixel vertex detector. The mass is defined as  $M = \sqrt{M_{ch}^2 + P_t^2} + |P_t|$ , where  $M_{ch}^2$  is the mass of the ensemble of charged tracks associated with the secondary vertex and  $P_t$  is the net transverse momentum with respect to the line connecting the secondary vertex and the IP. Charm candidates were required to have a vertex mass in the range  $0.55 < M_c < 2 \text{ GeV}/c^2$ . By vetoing on b-events and imposing momentum cuts charm events are isolated with 81% purity. Several methods are employed to determine the direction of the charm quark needed for the  $A_{FB-LR}$  evaluation, such as vertex charge,  $K^\pm$  tag, lepton tag and  $D^*$ ,  $D^+$  identification. These tags have different efficiencies in the range of  $\sim 30\%$ . A maximum likelihood fit to all tagged events is used to determine  $A_c$ .

Referring to Table 6, the  $A_c$  LEP-SLC average is in good agreement (only 0.6  $\sigma$ ) with the SM value of  $A_c = 0.668$  for  $\sin^2\theta_w^{eff} = 0.23155$  with the preliminary SLD value lower than the SM by about 0.5  $\sigma$  and the LEP value low by 0.9 $\sigma$ . The LEP values are derived from measurements which average to  $\langle A_{FB}^{0,c} \rangle = 0.0714 \pm 0.0044$ , corrected by  $4/(3 A_e)$ .

Table 6:  $A_c$  measurements from LEP and SLC (Summer-98).

Experiment	Method	$A_c$
SLD	K & vtx-Q	$0.65 \pm 0.04 \pm 0.03$
SLD	lepton	$0.70 \pm 0.09 \pm 0.07$
SLD	$D^*$ , $D^+$	$0.63 \pm 0.06 \pm 0.04$
SLD average		$0.649 \pm 0.040$

DELPHI	lepton	$0.73 \pm 0.10 \pm 0.11$
L3	lepton	$0.82 \pm 0.29 \pm 0.19$
ALEPH	D*	$0.63 \pm 0.08 \pm 0.02$
DELPHI	D*	$0.64 \pm 0.08 \pm 0.04$
OPAL	D*	$0.62 \pm 0.11 \pm 0.05$
LEP average		$0.634 \pm 0.040$
LEP+SLD average		$0.642 \pm 0.028$

A summary of measurements of  $A_b$  is shown in Table 7, where correlations were taken into account in the computation of averages. The SM predicts  $A_b = 0.935$  for  $\sin^2\theta_w^{eff} = 0.23155$  which is  $3.2 \sigma$  larger than the measurement world average. We note that the LEP and preliminary SLC values are consistent with the SLC value is  $1.9 \sigma$  lower than the SM and LEP is  $2.3 \sigma$  low.

Table 7:  $A_b$  measurements from LEP and SLC (Summer-98).

Experiment	Method	$A_b$
SLD	jet charge	$0.849 \pm 0.026 \pm 0.031$
SLD	lepton	$0.932 \pm 0.058 \pm 0.038$
SLD	$K^\pm$ tag	$0.854 \pm 0.088 \pm 0.106$
SLD average		$0.866 \pm 0.036$
ALEPH	lepton	$0.908 \pm 0.041 \pm 0.020$
DELPHI	lepton	$0.904 \pm 0.057 \pm 0.026$
L3	lepton	$0.869 \pm 0.055 \pm 0.030$
OPAL	lepton	$0.851 \pm 0.038 \pm 0.021$
ALEPH	jet charge	$0.953 \pm 0.037 \pm 0.029$
DELPHI	jet charge	$0.898 \pm 0.042 \pm 0.021$
L3	jet charge	$0.806 \pm 0.106 \pm 0.051$
OPAL	jet charge	$0.898 \pm 0.047 \pm 0.037$
LEP average		$0.885 \pm 0.022$
LEP+SLD average		$0.880 \pm 0.017$

The analysis of  $A_b$  involves many of the same considerations as discussed above for the extraction of  $A_c$ . A vertex mass tag is used, as in the case of  $A_c$ , but for the  $b\bar{b}$  events becomes more effective because the b-quark is heavier than any other visible quark and hence a large vertex mass which can be well separated from background. By requiring  $M_b > 2 \text{ GeV}/c^2$ , the b-quark purity is 97% with an efficiency of 76%. Several strategies are used to determine the direction of the b-quark, such as jet charge, lepton tag or a  $K^\pm$  tag which exploits the  $b \rightarrow c \rightarrow s$  decay cascade. All methods have to rely on Monte Carlo simulations to a greater or lesser extent. The jet charge method has the advantage in that it is self-calibrating. Again, the LEP values for  $A_b$  are derived from measurements of  $A_{FB}^{0,b}$  which have an average value of  $\langle A_{FB}^{0,b} \rangle = 0.0991 \pm 0.0021$ , and are corrected by the factor  $4/(3A_e)$ .

## 5.2 Measurements of $R_c$ and $R_b$

The  $Z^0$  branching fractions  $R_c$  and  $R_b$  are interesting places to search for violations of the SM. The largest known radiative corrections to  $R_b$  in the SM are charge-current vertex diagrams which are dominated by the top quark<sup>13</sup>. In the past,  $R_b$  has stirred considerable interest in that the measurements were in significant disagreement with the SM. In the summer of 1995, for example, the value of  $R_b$  was almost 4 standard deviations different from the SM. However, a new analysis presented at ICHEP'96 by ALEPH<sup>14</sup>, which, among several improvements, reduced hemisphere correlations by reconstructing the primary vertex in each hemisphere for each event, resulted in a precise value of  $R_b$  in close agreement with the SM.

Tables 8 and 9 summarize the  $R_c$  and  $R_b$  measurements, respectively, from LEP<sup>8</sup> and SLC<sup>15, 16</sup>. A double tag method is used in both the  $R_c$  and  $R_b$  analyses where the heavy quark tagging procedure outlined above is applied independently to each thrust hemisphere of all hadronic events. Determining the single tag, double tag and mixed tag rates enables the tagging probability to be estimated by the data itself.

Table 8: Measurements of  $R_c$  (Winter-98).

Experiment	Method	$R_c$
SLD	VTX-mass	$0.1794 \pm 0.0085 \pm 0.0061$
ALEPH	lepton	$0.168 \pm 0.006 \pm 0.010$
DELPHI	lepton	$0.164 \pm 0.009 \pm 0.020$
ALEPH	c-counting	$0.176 \pm 0.005 \pm 0.011$
DELPHI	c-counting	$0.168 \pm 0.011 \pm 0.013$
OPAL	c-counting	$0.167 \pm 0.011 \pm 0.011$
ALEPH	D* incl/excl	$0.166 \pm 0.012 \pm 0.009$
DELPHI	D* incl/excl	$0.176 \pm 0.015 \pm 0.015$
OPAL	D* incl/excl	$0.180 \pm 0.011 \pm 0.013$
ALEPH	D* excl/excl	$0.173 \pm 0.014 \pm 0.009$
DELPHI	D* incl/incl	$0.171 \pm 0.013 \pm 0.015$
SLD+LEP average		$0.1731 \pm 0.0044$

A set of equations is developed in which either  $R_c$  or  $R_b$  can be determined which

avoids large uncertainties of a direct calculation of the single tag efficiency. The b-tagging efficiency is typically  $\epsilon_b \sim 35\%$  with a hemisphere correlation of  $\lambda_b \sim 0.6\%$ .

The  $R_c$  world average is within  $0.2\sigma$  of the SM value of  $R_c = 0.1723$ . The SLD values are consider preliminary. The  $R_b$  world average of Table 9 is within  $1.4\sigma$  of the SM value of  $R_b = 0.2155$ . Hence the interesting  $4\sigma$  discrepancy with the SM of the summer 1995 has dissolved into fairly good agreement.

Table 9: Measurements of  $R_b$  (Summer-98).

Experiment	Method	$R_b$
SLD (prelim.)	VTX+mass	$0.2159 \pm 0.0014 \pm 0.0014$
ALEPH	multi-var	$0.2159 \pm 0.0009 \pm 0.0011$
DELPHI	multi-var	$0.2163 \pm 0.0007 \pm 0.0006$
L3	impact+lept	$0.2176 \pm 0.0015 \pm 0.0026$
OPAL	VTX+lept	$0.2176 \pm 0.0011 \pm 0.0014$
LEP+SLD average		$0.21656 \pm 0.00074$

### 5.3 Comment on $A_b$ and $\sin^2\theta_w^{eff}$

$A_b$  itself shows the same difference as we observed in the  $\sin^2\theta_w^{eff}$  value derived from  $A_{FB}^{0,b}$  above - namely  $A_{FB}^{0,b}$  measured is smaller than the prediction of the SM, resulting in a larger value of  $\sin^2\theta_w^{eff}$  from the LEP measurements. Remember that we have used the pure leptonic determination of  $A_e$  to correct the LEP forward-backward asymmetries in order to obtain the value of  $A_b$  by the factor  $4/(3A_e)$ . Also note that the SLD measures  $A_b$  directly by means of the forward-backward left-right asymmetry.

Examining the factors involved we conclude that the discrepancy in  $\sin^2\theta_w^{eff}$  between LEP and the SLD is consistent with a discrepancy of the value of  $A_b$  from the SM. In fact, if we take the direct measurement of  $A_b$  from the SLD to derive the value of  $A_e$  from the LEP value of  $A_{FB}^{0,b}$  we obtain a value of  $\sin^2\theta_w^{eff}$  which is *consistent with the pure leptonic value*. The equation below show this calculation.

$$A_e = \frac{4}{3} \frac{A_{FB}^{0,b}(\text{LEP})}{A_b(\text{SLD})} = \frac{4}{3} \frac{0.0991 \pm 0.0021}{0.866 \pm 0.036} = 0.1526 \pm 0.0071, \quad (12)$$

which results in  $\sin^2\theta_w^{eff} = 0.2308 \pm 0.0009$  - in good agreement ( $0.5 \sigma$ ) with the pure leptonic value of  $\sin^2\theta_w^{eff} = 0.23127 \pm 0.00023$ . If the value  $A_b(\text{LEP}) = 0.885 \pm 0.022$  (completely correlated with  $A_{FB}^{0,b}$ ) is used instead  $\sin^2\theta_w^{eff} = 0.23112 \pm 0.00038$ .

In a more sophisticated context, the analysis of Takeuchi, Grant and Rosner<sup>17</sup> shows that the data of LEP and SLD are consistent in the pure leptonic sector and that the (current) major discrepancy ( $3.2 \sigma$  too low) is in the value of  $A_b$ . The left-handed coupling of the b-quark is tightly constrained by  $R_b$  and is in agreement the SM.  $A_b$  is sensitive primarily to the right-handed coupling and is not in agreement with the SM. (See eqs. 11.) Fig. 4 shows the analysis of the current experimental situation.

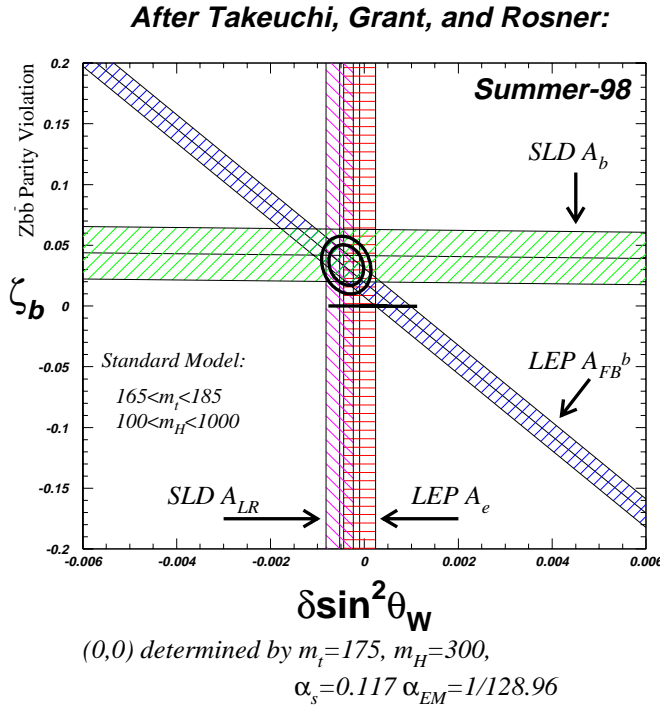


Figure 4: The consistency of the world's data is shown by the overlap of the measurement bands. The inconsistency with the SM is indicated by the offset of the

overlap of measurements with the expectation of the SM given by the (0,0) point of the figure.

The TGR<sup>17</sup> variable  $\zeta_b$  is sensitive to the parity violation of the b-quark, as measured by  $A_b$ . Its value is insensitive to the value of  $\sin^2\theta_w^{eff}$ . Hence the horizontal band in Fig.4.  $A_{LR}$  and LEP  $A_e$  are most strongly dependent on  $\sin^2\theta_w^{eff}$  - hence the vertical bands.

## 7 Radiative Corrections

We have observed that the data of LEP and SLD generally agree with the predictions of the standard model, although there is some concern over the discrepancy of  $A_b$ , and consequently the value of  $\sin^2\theta_w^{eff}$  derived from the b-quark sector. So far we have checked that eq. 3 is generally valid, namely that the vector and axial vector couplings of a fermion to the  $Z^0$  - boson follow the weak isospin assignments and depend on the electric charge and effective weak mixing angle in a universal way. This is a test of the  $SU(2)_L \times U(1)$  gauge structure of the theory.

In order to check the theory beyond the 'tree level' radiative corrections must be included. This process is usually performed by fitting all the measured quantities at the  $Z^0$ -pole with radiative corrections to derive the top quark mass and the Higgs mass, or constraining the top quark mass by the measured value at FNAL and deriving the Higgs mass. The consistency of the theory is measured by the quality of the fit. Sensitivities to  $M_t$  and  $M_h$  arise from different measured quantities having different dependencies on the parameters of the radiative corrections. Already we have absorbed the vertex corrections for lepton (but not for quarks) by defining an effective mixing angle determined by  $A_e$ , the electron coupling constant asymmetry.

There have been a number of theoretical treatments which make the comparison of theory to data less model-dependent<sup>18</sup>. Here we adopt a more pedestrian approach and use 'experimental' parameters, such as  $M_t$  and  $M_h$  to obtain an estimate of the magnitude of various terms. The need for radiative corrections is easily demonstrated in a naive evaluation of eq. 2 using the value of  $\sin^2\theta_w^{eff}$  determined above,  $\alpha_{em}$  given by atomic physics experiments and  $G_F$  from muon decay. This naive exercise predicts  $M_Z = 88.38 \pm 0.03$  GeV and  $M_W = 77.48 \pm 0.04$  GeV, values which are embarrassingly discrepant with the measured values of  $91.1867 \pm 0.0021$  GeV and  $80.37 \pm 0.090$  GeV, respectively [Vancouver 1998]<sup>8</sup>.

Radiative corrections are grouped into two general types: (1) electromagnetic corrections, which include initial and final state radiation, vertex diagrams, etc. and the running of  $\alpha_{\text{em}}$  for the atomic energy scale  $q^2 \cdot 0$  to the  $q^2 = M_Z^2$ ; and (2) electroweak corrections where some of the corrections are absorbed in the definition of  $\sin^2\theta_w^{\text{eff}}$ , isospin-breaking loop terms in W and Z propagators, running of Z self-energy, corrections to the  $Z \rightarrow b \bar{b}$  vertex and corrections to the W mass.

## 7.1 Hadronic Vacuum Polarization

Much of the discrepancy in the vector boson mass relations is corrected by the running of  $\alpha_{\text{em}}(Q^2)$ . The QED coupling at the  $M_Z$  scale is related to its value at low energy, given precisely in atomic physics experiments by

$$\alpha_{\text{em}}(M_Z^2) = \frac{\alpha_{\text{em}}(0)}{1 - \Delta\alpha_{\text{em}}(M_Z^2)}, \quad (13)$$

where  $\Delta\alpha_{\text{em}}(M_Z^2) = -\Pi_{\gamma\gamma}$  is the photon self-energy. The photon self-energy is evaluated quite accurately for leptons, but not for quarks. In order to evaluate the quark contribution the measured  $e^+ e^-$  hadronic cross section is employed to determine the value of a dispersion integral. Ironically, the data in the 1.05 to 5 GeV region, well beneath the scale of the  $Z^0$ -pole, contribute a large fraction of the integral as well as large part of the uncertainty. Much of the data in this energy region are old and have large normalization errors. Further, above the charm threshold, many channels with different properties exist, complicating the evaluation of the integral. A number of evaluations have been performed<sup>19</sup>. The result adopted by the LEP EW-WG is  $\alpha_{\text{em}}(M_Z^2) = 1 / 128.896 \pm 0.090$  which is an evolution of  $\Delta\alpha / \alpha \sim 0.063$ . In this formulation  $G_F$ , does not run<sup>20</sup>.

## 7.2 Electroweak Radiative Corrections

The radiative corrections are furnished by the terms  $\zeta$  in eqs. 2 and 5 above. At the one-loop level the correction terms for the  $M_Z$  mass relation given by eq. 2a is

$$\zeta_Z = (1 + \Delta\rho) (1 + \Delta_{3Q}), \quad (14a)$$

where, for leading order with  $M_t = 175$  GeV and  $M_h = 160$  GeV, the isospin-breaking

loop correction to the  $W^\pm$  and Z propagators and Z self-energy terms, respectively, are

$$\Delta\rho \approx \frac{\alpha}{\pi} \frac{M_t^2}{M_Z^2} - \frac{\alpha}{4\pi} \ln \frac{M_h^2}{M_Z^2} \sim 0.0084 \quad (14b)$$

$$\Delta_{3Q} \approx \frac{\alpha}{9\pi} \ln \frac{M_h^2}{M_Z^2} \sim 0.00031. \quad (14c)$$

The overall electroweak correction to the Z-mass relation is dominated by the quadratic  $M_t$  term and has the magnitude,  $\Delta\zeta_Z/\zeta_Z \sim 0.0087$ . The corresponding correction for  $M_W$  (eq. 2b) is

$$\zeta_W = 1 - \Delta r_{ew} \quad (15a)$$

where

$$\Delta r_{ew} \approx - \frac{c_0^2}{s_0^2} \Delta\rho \sim -0.028 \quad (15b)$$

with  $s_0^2 c_0^2 = \pi \alpha_{em}(M_Z^2) / \sqrt{2} G_F M_Z^2$  yielding  $\Delta\zeta_W/\zeta_W \sim 0.028$ . The correction to the  $Z^0 \rightarrow b \bar{b}$  partial width is given by

$$\zeta_{b\bar{b}} = (1 + \delta_{QCD})(1 + \delta_{vb}). \quad (16a)$$

The QCD component to next-to-leading order is

$$\delta_{QCD} \approx \frac{\alpha_s(M_Z^2)}{\pi} + 1.41 \left( \frac{\alpha_s(M_Z^2)}{\pi} \right)^2 \sim 0.038 \quad (16b)$$

for  $\alpha_s(M_Z^2) = 0.12$ . The vertex correction,  $\delta_{vb}$ , is

$$\delta_{vb} \approx - \frac{20}{13} \frac{\alpha}{\pi} \left( \frac{M_t^2}{M_Z^2} + \frac{13}{6} \ln \frac{M_t^2}{M_Z^2} \right) \sim -0.025. \quad (16c)$$

In addition to the QCD and vertex corrections for  $\Gamma_{bb}$  there are QED and finite mass terms. From the list above the largest correction to the mass relations of eqs. 2 is the running of  $\alpha_{em}$  from the atomic scale to the  $M_Z$  scale. Other corrections are quadratic in  $M_t$ , and logarithmic in  $M_h$ . Two-loop electroweak top corrections are being reconsidered<sup>21</sup> and may be important.

## 8 Global Test of the Standard Model

Within the context of the SM different electroweak observables are sensitive to different radiative correction parameters ( $M_t$ ,  $M_h$ ,  $\alpha_s$ ). For example,  $R_b$  has a strong sensitivity to  $M_t$  and little to  $M_h$ ,  $M_w$  is sensitive to both  $M_t$  and  $M_h$  and  $\sigma_{had}^0$  depends on  $\alpha_s$ . These different sensitivities are exploited to determine the value of  $M_t$  and set limits on  $M_h$  or with a constrained value of  $M_t$  determine (still within large errors) the value of  $M_h$ . Table 10 shows the results of a fit (ZFITTER 5.10)<sup>22</sup> to all the world's electroweak data [  $M_w$ ,  $R_v$ ,  $\Gamma_z$ ,  $\sigma_{had}^0$ ,  $R_l$ ,  $A_{FB}^l$ ,  $A_e$ ,  $A_t$ ,  $A_{LR}$ ,  $A_{FB}^b$ ,  $A_{FB}^c$ ,  $R_b$ ,  $R_c$ ,  $Q_{FB}$ ,  $Q_w(Cs)$  and  $Q_w(Tl)$  ].

Table 10: Results of a fit to electroweak data at  $Z^0$ -pole.

Parameter	Constraint	Best Fit
$M_Z$ (GeV)	$91.187 \pm 0.002$	91.187
$1/\alpha_{em}(M_Z^2)$	$128.928 \pm 0.023$	$128.928 \pm 0.023$
$M_t$ (GeV)	$173.8 \pm 5.0$	$172.2 \pm 4.8$
$\alpha_s(M_Z^2)$	-----	$0.119 \pm 0.003$
$\log_{10}(M_h)$	-----	$1.981^{+0.216}_{-0.242}$
$M_h$ (GeV)	-----	$95.6^{+61.6}_{-40.9}$

$\chi^2/\text{DoF}$	-----	15.2/14 (37%)
---------------------	-------	---------------

The fitted value of  $M_t$  is in agreement with the direct observation at FNAL<sup>23</sup>  $M_t = 173.8 \pm 5.0$  GeV. The limits on  $M_h$  are  $> 90$  GeV from direct searches and  $< 280$  GeV at 95% CL<sup>24</sup>.

It is interesting to note that the SLD value of  $\sin^2\theta_w^{eff}$  implies a Minimal Standard Model (MSM) Higgs scalar of  $\sim 40$  GeV and is  $\sim 1 \sigma$  in contradiction with the present direct search limit of  $> 90$  GeV at the 95% CL, whereas the LEP value is consistent with  $M_h \sim 220$  GeV and is not excluded by direct searches.

A more sophisticated way of looking the data is shown in Figure 5 as a comparison of the world's data with the variables S and T of Peskin and Takeuchi<sup>25</sup>. The variables S and T are normalized to (0,0) at a nominal SM point - determined by the measured value of  $M_t$  and a nominal value of  $M_h$ . The contributions to isospin-violating mass differences beyond the set point are described by T which is roughly quadratic in  $M_t$  and logarithmic in  $M_h$  (see eqs. 14 and 15 above). The parameter S is sensitive to isospin-independent terms which would grow systematically with the size of a new sector. The Peskin-Takeuchi variable U is assumed to be 0 in this application. The 68% confidence region of the LEP and SLD data is indicated by the oval region in the figure.

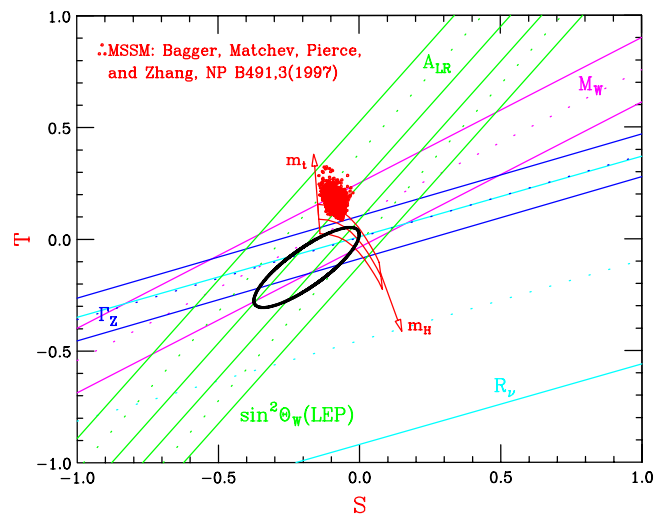


Figure 5: The S and T constraints provided by LEP, SLD and FNAL are indicated. The SLD measurement of  $A_{LR}$  seem to prefer the MSSM of Pierce, et al.<sup>26</sup>.

The S-T region predicted by the MSM is indicated by the "banana-region" centered about the (0,0) point of the figure. In that region, the right-hand edge corresponds to  $M_h = 88$  GeV and  $M_t = 173.9 \pm 5.2$  GeV. Increasing the Higgs mass up to 1 TeV is displayed by the width of the region. An indication of supersymmetry would be a shift of the experimental overlap region from the expectations of the MSM with S becoming slightly negative and T positive. The MSSM of Pierce, et al.<sup>26</sup> is indicated by the ensemble of dots in the figure - each representing a choice of the five parameters of the model. We note the SLD data<sup>27</sup> favors a super-symmetric world, whereas LEP data disfavors the model by about  $2\sigma$ .

## 9 Summary and Conclusions

The Standard Model works remarkably well with only one parameter,  $A_b$ , out of some 18 measurements differing significantly for theory prediction<sup>28</sup>. The  $SU(2)_L \times U(1)$  structure of the theory is quite well established though one-loop electroweak radiative corrections, although the b-quark sector continues to exhibit troublesome inconsistencies. The largest discrepancies are  $\Delta \sin^2 \theta_w^{eff}$  (SLD vs. LEP)  $\sim 2.2\sigma$  and  $\Delta A_b$  (SLD+LEP vs. SM)  $\sim 3.2\sigma$ . Most of the  $\Delta \sin^2 \theta_w^{eff}$  (SLD vs. LEP) is resolved by considering only purely leptonic determinations of the electroweak mixing angle, isolating the puzzle of why  $A_b$  does not agree with the SM. Analyses of  $A_b$  are involved and, to a greater or lesser extent, rely on Monte Carlo simulation to estimate the experimental resolution, efficiency and background. These simulations may be flawed in a subtle way and therefore contribute to the discrepancy - or there may be 'new' physics at long last becoming visible in the b-sector. If the purely leptonic value (SLD and LEP) of  $\sin^2 \theta_w^{eff}$  is ultimately preferred then the precision electroweak data suggest that the Higgs scalar is light and direct search searches for it become quite tantalizing.

The SLD has proposed to take more data at the  $Z^0$ -pole which will continue to probe the SM, especially in refining the measurement of  $\sin^2 \theta_w^{eff}$  and b-quark parameters. Data from LEP-II will decrease the uncertainty in  $M_W$ , explore the triple vertex

coupling and search for exotic particles beyond the SM. FNAL Run-II at FNAL will decrease the  $M_t$  and  $M_W$  errors. And 'modern' low energy data (Novosibirsk, BES, DAPHNE, B-factories) should improve the evaluation of  $\Delta\alpha_{\text{em}}(M_Z^2)$  and sharpen the radiative corrections.

## Acknowledgments

I would like to thank the organizers and participants of this conference for a very stimulating time. Special thanks go to my SLD colleagues and to the SLC Accelerator Department for their outstanding performance.

## References

- [1] M. Breidenbach, SLAC-PUB-3798 (1985); K. Abe, et al. Phys. Rev. D53 (1996) 1023; M. Woods, SLAC PUB-7320 (1996); E. Torrence, SLAC-REPORT-509 (1997); A. Lath, SLAC-REPORT-454 (1994).
- [2] K. Abe et al., Nucl. Inst. and Meth., A400, (1997), 287-343.
- [3] S. Weinberg, Phys. Rev. Lett. 19 (1967) 1264; A. Salam, in *Elementary Particle Theory*, ed. N. Svartholm p.367.
- [4] See for example: D.C. Kennedy and B.W. Lynn, Nucl. Phys. B322 (1989), 1.
- [5] K. Abe, et al. Phys. Rev. Lett. 78 (1997) 2075-2079.
- [6] K. Abe, et al. Phys. Rev. Lett. 79, 804-808 (1997); R.S. Panvini, SLAC-PUB-7375; A. K. McKemey, Proc. ICHEP'96.
- [7] K. Abe et al., SLAC-PUB-7878 (1998).
- [8] For recent LEP data see M. Martinez, *Precision Electroweak Results at LEP I and LEP II*, in Proc. this Conference (Stanford, CA) 1998; See also D. Abbaneo, et al. ElectroWeak Working Group, Internal Memo LEPEWWG/97-01; CERN-PPE/97-154; J. Timmermans, in *Proc. XVIII Int. Sym. on Lepton-Photon Int.*, Hamburg (1997).
- [9] SLD  $A_S$ : K. Abe, et al., SLAC-PUB-7825 (1998).
- [10] SLD  $A_C$ : K. Abe, et al., SLAC-PUB-7879 (1998).
- [11]  $A_B$  analyses from the SLD are discussed in K. Abe, et al., SLAC-PUB-7886 (1998); K. Abe, et al. SLAC-PUB-7959 (1998); See also Dong Su, in "Heavy

Quark Couplings to the  $Z^0$ , presented at the *XVIII International Symposium on Lepton Photon Interactions*, (1997), Hamburg, Germany.

- [12] D. Jackson, Nucl. Inst. and Meth., A338, (1997) 247.
- [13] See for example: A. Blondel and C. Verzegnassi, Phys. Lett. B 311 (1993) 346-356.
- [14] ALEPH: Tomalin, I.R.; in *Proc. of ICHEP'96*, Warsaw, Poland, p1340 (1996).
- [15] SLD  $R_c$ : K. Abe, et al. SLAC-PUB-7880 (1998).
- [16] SLD  $R_b$ : K. Abe, et al. Phys. Rev. Lett. 80 (1997) 660.
- [17] T. Takeuchi, A. Grant, J. Rosner, p. 1231 in *Proc. of 8<sup>th</sup> Meeting of the DPF* (Albuquerque, N.M. 1994), S. Seidel, ed.
- [18] G. Altarelli, R. Barbieri, S. Jadach NP B369, 3, (1992); W. Marciano, in *Proc. of this Conf.* Stanford, CA (1998).
- [19] M. Swartz, SLAC Pub 95-7001; H. Burkhardt, B. Pietrzyk, LAPP-Exp-95.05.
- [20] R.D. Peccei, DESY 89-060.
- [21] G. Degrassi, et al., hep-ph/9412380.
- [22] The fit uses ZFITTER, D. Bardin, et al., CERN-TH 6443/92 (May 1992); hep-ph/9412201.
- [23] See R. Brock, in *Proc. of Fund. Particles and Interactions*, p. 189, Nashville, TN, R.S. Panvini and T.J. Weiler, Eds. (1997); J. Kotcher, in *Proc. this Conf.* Stanford, CA (1998).
- [24] D. Karlen, ICHEP'98, Vancouver, BC (1998).
- [25] M. Peskin and T. Takeuchi, Phys. Rev. D46, 381-409 (1992).
- [26] D. Pierce, et al., Nucl. Phys. B 491 (1997) 3-67.
- [27] "Request for SLD Run Extention", SLD Collaboration (Aug. 1998).
- [28] An earlier comparison of LEP-SLC data can be found in F.E. Taylor, in *Proc. of Fund. Particles and Interactions*, p. 166, Nashville, TN, R.S. Panvini and T.J. Weiler, Eds. (1997).